

Quantile-quantile Correction of Satellite-based Relative Productivity in Northern Tunisia

Nesrine ABID✉ and Zoubeida BARGAOUI

University Tunis El Manar, National School of Engineers of Tunis (ENIT),
Hydraulics and Environment Laboratory (LMHE), Tunis, Tunisia

✉ nesrine_abid@ymail.com

Abstract

Satellite products such as normalized difference vegetation index (NDVI), the fraction of vegetation cover (FVC), and evapotranspiration are worth to drought assessment and alert. We consider time series of SPOT vegetation NDVI and FVC, as well as Satellite Application Facility on Land Surface Analysis (LSA SAF), reference evapotranspiration ET_0 to estimate potential evapotranspiration E_p at 3 km resolution and 10-days' time step in northern Tunisia. In addition, based on satellite LSA SAF observations of actual evapotranspiration E , we produce maps of the ratio E/E_p or relative productivity. To analyze drought conditions, we consider the time horizon from January to May relevant for cereal crops. Resulting relative productivity maps are then compared to field evidence relative to areas damaged by drought. Bias correction method is then used to correct relative productivity cumulative distribution. Results show that two thresholds are required to correct relative productivity maps to assign zero for low levels and one for high levels of relative productivity. In addition, quantile-quantile regression is worth completing relative productivity map correction.

Keywords: drought, remote sensing data, evapotranspiration, relative productivity.

1. INTRODUCTION

Drought assessment is helpful for crop yield estimation and has repercussions on the country's trade balance and food security. Satellite products are worth for assessing drought occurrence and severity. While satellite products are worth at a regional scale, they need to be analyzed at a local scale. Different methods are used for such assessment. In different parts of the world, flux tower data were used to verify the accuracy of actual evapotranspiration using as reported

from satellite observations (Cleugh et al. 2007; Paca et al. 2019). Here we propose to compare remote-sensing estimated evapotranspiration under drought conditions, with field evidence of crop damage (Abid et al. 2018). Tunisia's economy is vulnerable to drought and particularly cereal crop droughts. That's why it is challenging to use satellite products to help monitor drought and crop yield in Tunisia (Zribi et al. 2016; Chakroun 2017).

2. MATERIAL AND METHODS

2.1 Material

The study area is northern Tunisia mainly composed of three core watersheds (North Mediterranean facade watersheds called basin 3; the Medjerda basin called basin 5, and the East facade Cap-Bon and Meliane river basins called basin 4). This area covers 346 378 km². Climate conditions vary from higher humid to lower semi-arid according to Emberger index. Vegetation is composed of forest, cropland, and sparse vegetation. The study region is decomposed into 1101 units which are local administrative units called "Imada". Only 777 out of them that are non-urban areas are considered for remote-sensing estimates and field comparison. Field evidence data are obtained by analyzing the Official Journal of the Tunisian Republic where are published for each Imada the percentage of drought-damaged areas for every cereal crop campaign considering the time step from September to next May. We selected the crop campaign of 2015–2016 which is characterized by a drought that threatened more than 60% of the study area (Fig. 1). We use the variable F_a which is related to the area damaged by cereal crop drought. $F_a = 1$ returns for zero percent of the Imada's area is affected by cereal crop drought while $F_a = 0$ returns for 100 percent of the Imada's area is affected by cereal crop drought. For the period September 2015 to May 2016, we download fraction of vegetation cover FVC and normalized difference of vegetation index NDVI observations from the Copernicus SPOT-

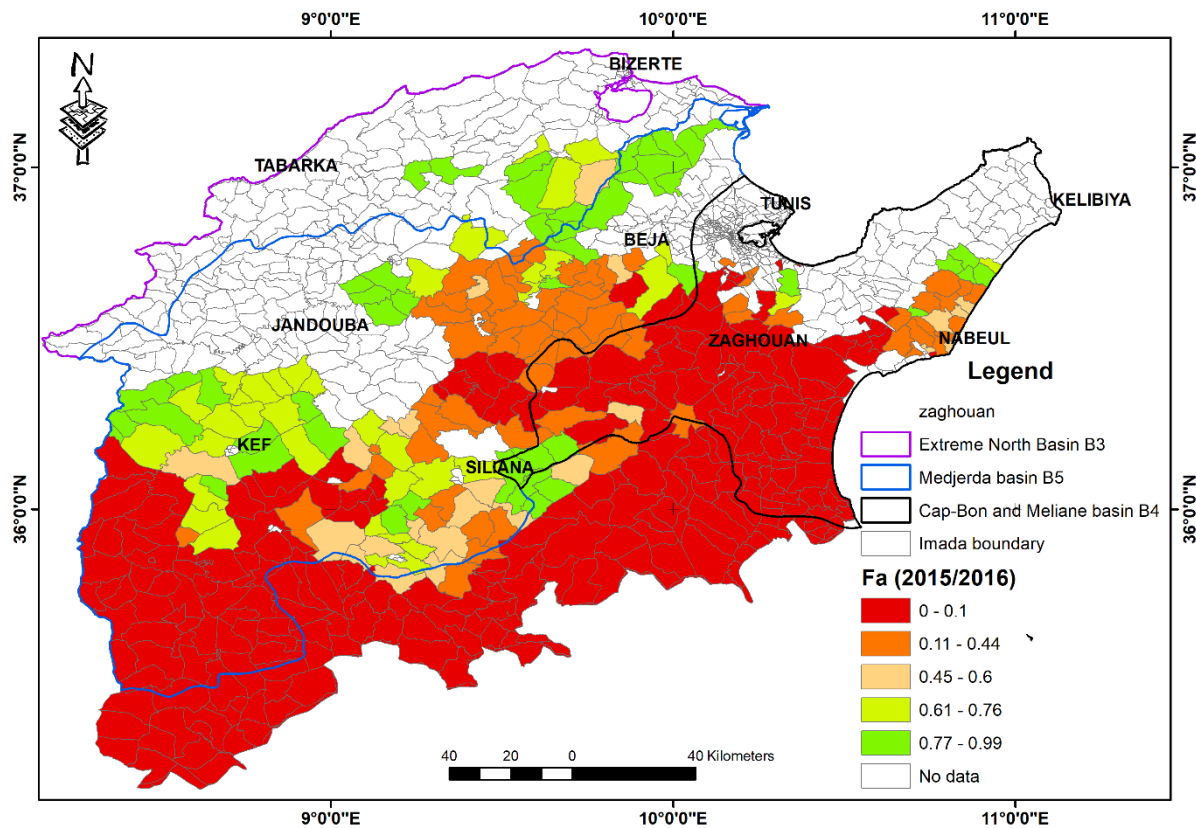


Fig. 1. Map of F_a for the 2015–2016 crop campaign.

Vegetation product with a 10-day time resolution and 1 km spatial resolution. In addition, we download actual evapotranspiration E and reference evapotranspiration ET_0 from LSA SAF products. The time resolution is daily, and the spatial resolution is 3 km. Daily E as well as daily ET_0 series are summed to obtain the totals for the period January to May 2016. Then, they are averaged over administrative entities (Imadas).

2.2 Methods

According to Eagleson (1994), for a column of atmosphere and soil of unit width, assuming the climate to be stationary, and time averaging the differential water balance equation, one obtains the climatic water balance equation:

$$P - E(S/\text{climate, soil}, M, k_v) - R(S/\text{climate, soil}) = 0 \quad , \quad (1)$$

where P is the average yearly precipitation received by the surface, E – average yearly actual evapotranspiration, M – fraction of the surface covered by vegetation or canopy density, R – average yearly surface runoff, S – soil moisture state, k_v is the ratio $k_v = E/Ep$, and Ep is potential evapotranspiration also called relative productivity or crop efficiency or water stress coefficient.

As mentioned by Eagleson (1994), there are three types of functions describing productivity change versus environmental stress ($S-1$) distinguishing desert annual grasses and humid climate trees (Type 1) from semi-arid and subhumid trees and shrubs (Type 2) and from perennial desert plants (Type 3). Type 2's k_v varies roughly between 0.4 and 0.6 for conditions without or with small environmental stress and decreases abruptly to zero under environmental stress conditions. On the contrary, for Type 3 the null or small stress conditions is around 0.3 while it is around 0.9 for Type 1 signifying that atmospheric demand can be met. Thus, the transpiration is much restricted for Type 3 vegetation to cope with prolonged dry periods. We assume that under semi-arid conditions of northern Tunisia Type 2 behavior holds. These permits rescaling the satellite-derived E/Ep maps using two thresholds for relative productivity. Any satellite estimated k_v less than k_{vmin} is transformed to zero. Any satellite estimated k_v greater than k_{vmax} is transformed to 1. Thus, $F_a = 0$ corresponds to $k_v = 0$ and $F_a = 1$ corresponds to $k_v = 1$. Then, a regression is fitted between non-transformed sample quantiles of satellite-based k_v and the fraction F_a .

We estimate the crop coefficient K_c based on the FAO-56 dual crop coefficient approach (Allen et al. 1998) which is commonly used in the literature (Er-Raki et al. 2010). K_c is calculated as a function of K_{cb} and K_e (Rocha et al. 2010; Abid et al. 2018):

$$K_c = K_{cb} + K_e \quad , \quad (2)$$

where K_{cb} is crop transpiration coefficient, K_e – soil evaporation fraction, K_{cb} – a function of NDVI, and K_e is a function of FVC (Rocha et al. 2010; Abid et al. 2018).

The potential evapotranspiration is evaluated using Eq. (3):

$$E_p = K_c * ET_0 \quad . \quad (3)$$

Pixels E_p are first summed to obtain the January to May 2016 totals. Then, they are averaged over administrative entities (Imadas) and the ratio E/E_p is estimated for every entity. Its relevance is assessed in comparison to the fraction F_a informing about the percent of the area damaged by drought for cereal crops ($F_a = 0$ corresponds to 100% of the Imada affected by cereal crops). A statistical analysis of the sample cumulative distribution of F_a and satellite-based k_v is undertaken. Bias correction is achieved using the two above mentioned thresholds for satellite-based k_v as well as quantile-quantile regression (Piani et al. 2010).

3. RESULTS

Figure 2 shows the scatterplot of actual evapotranspiration averaged by Imada in comparison to potential evapotranspiration. Per Imada, in the period January–May 2016 total actual evapotranspiration vary between 20 and 200 mm while potential evapotranspiration is between 175 and 300 mm. Figure 3 shows the map of estimated k_v for the period from January to May 2016.

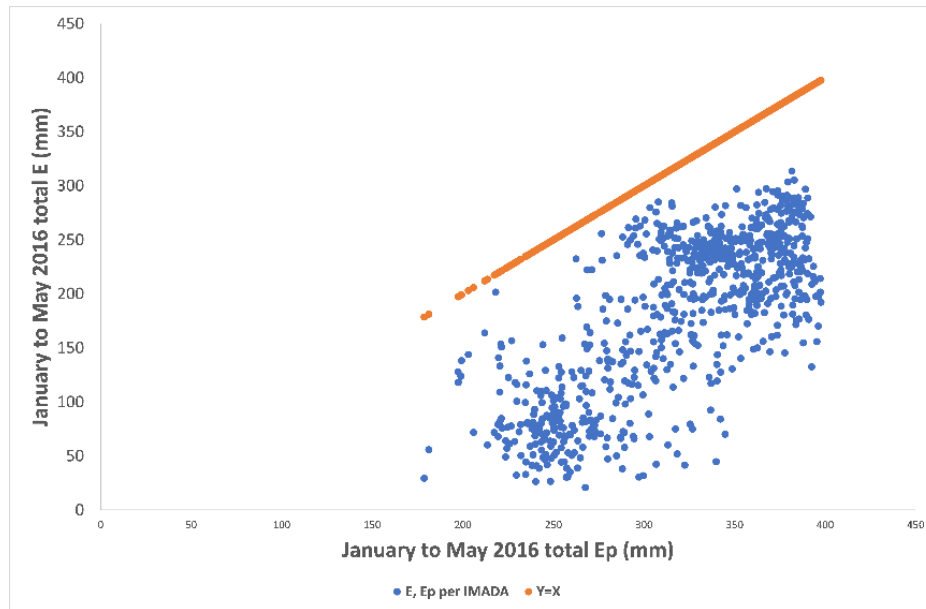


Fig. 2. Scatter plot for actual and potential evapotranspiration (January to May 2016) per Imada.

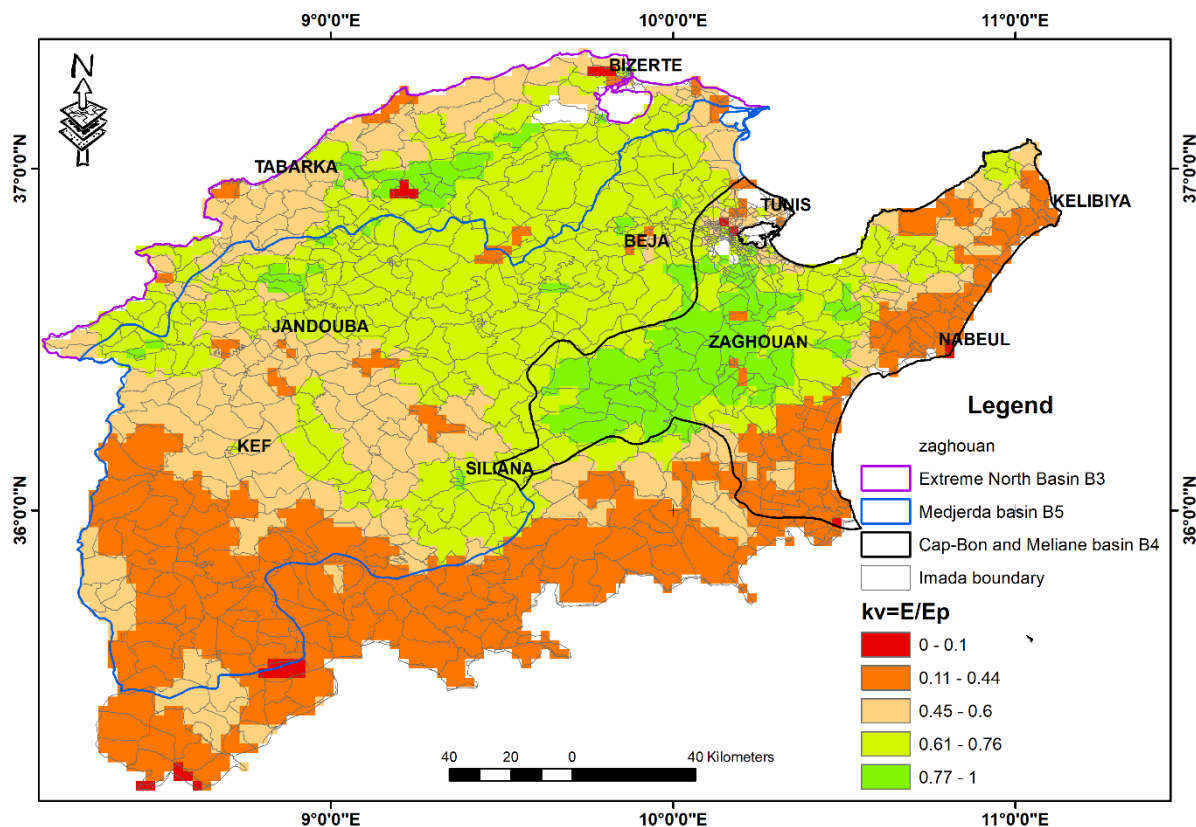


Fig. 3. Spatial distributions of k_v .

The sample distributions of ranked k_v and F_a are shown in Fig. 4. There is clearly a need for bias correction. Based on Fig. 4, the following thresholds are assumed: $k_{vmin} = 0.45$ and $k_{vmax} = 0.62$. Thus, for every Imada with raw $k_v < 0.45$ the transformed $k_v = 0$. Similarly, for every Imada with raw $k_v > 0.62$ the transformed $k_v = 1$. Otherwise, raw k_v are ranked as well as corresponding F_a . Quantile-quantile regression is then achieved (Fig. 5). As seen in Fig. 5, the regression is with very good accuracy helping drought impact investigation in northern Tunisia.

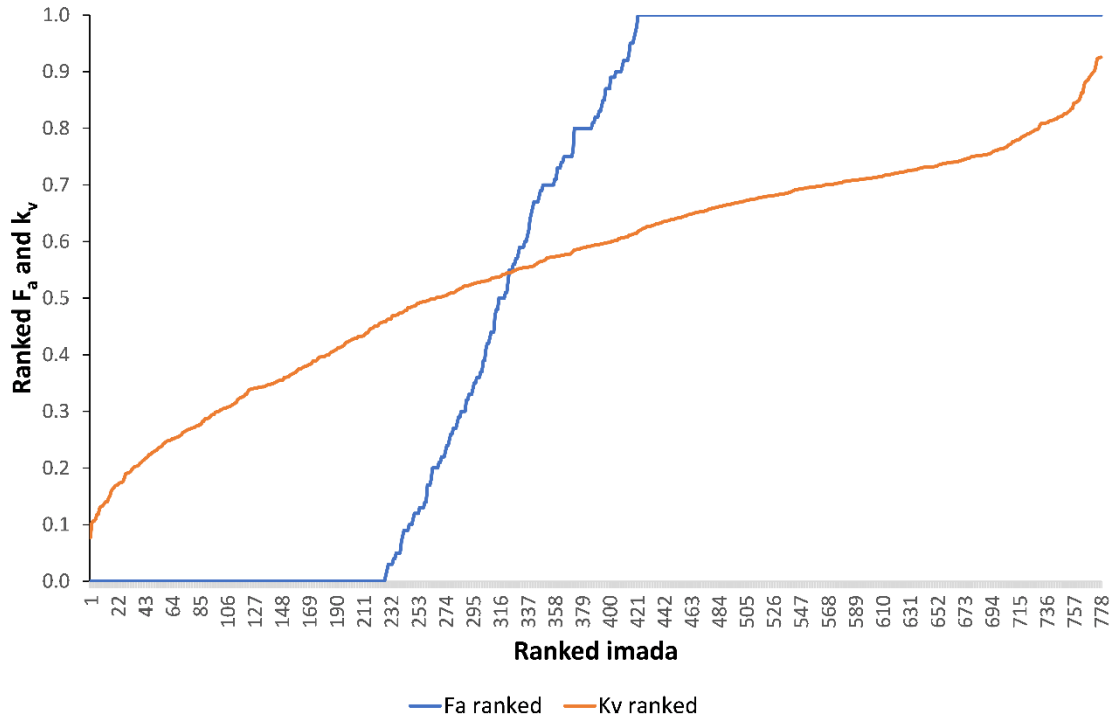


Fig. 4. Cumulative distributions of F_a and raw k_v .

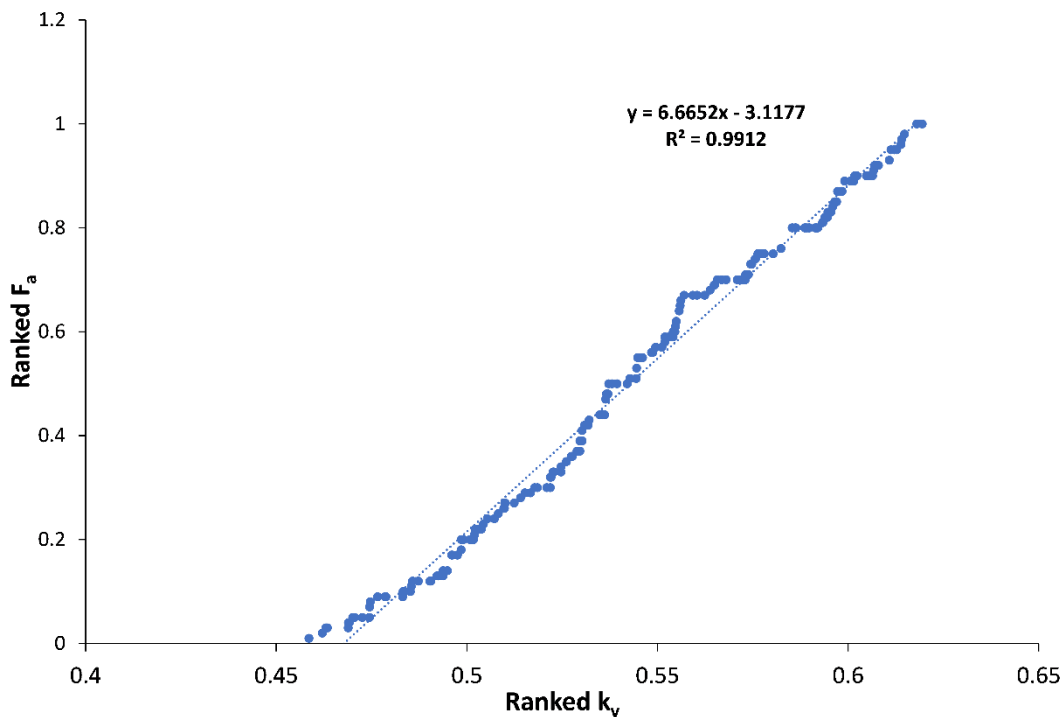


Fig. 5. Quantile-quantile regression between F_a and non-transformed k_v .

4. CONCLUSION

For Northern Tunisia and the drought occurred in the crop campaign 2015–2016, the field assessment achieved by the Tunisian authorities to estimate the percentage of the affected area by drought for every administrative unity at the local scale (Imada), is compared to the crop productivity calculated using remote sensing data and products from SPOT and LSA SAF. Bias correction using quantile-quantile regression resulted in a very good accuracy between the two derived maps. Therefore, the perspective is to evaluate the relevance of other periods for drought mitigation as well as to analyze other drought events and non-drought periods.

Acknowledgments. This work is under the national project PAQ-Collabora entitled “Monitoring/development of drought indices for decision support concerning the management of cereal productivity in Tunisia”. We thank the Ministry of High Education for this funding.

References

- Abid, N., Z. Bargaoui, and C.M. Mannaerts (2018), Remote sensing estimation of the water stress coefficient and comparison with drought evidence, *Int. J. Remote Sens.* **39**, 14, 4616–4639, DOI: 10.1080/01431161.2018.1430917.
- Allen, R.G., L.S. Pereira, D. Raes, and M. Smith (1998), Crop evapotranspiration – Guidelines for computing crop water requirements, FAO Irrigation and Drainage, Paper no. 56, FAO Rome, available at: <http://www.fao.org/docrep/X0490E/X0490E00.html>.
- Chakroun, H. (2017), Quality assessment of MODIS time series images and the effect on drought monitoring, *Open J. Appl. Sci.* **7**, 7, 365–383, DOI: 10.4236/ojapps.2017.77029.
- Cleugh, H.A., R. Leuning, Q. Mu, and S.W. Running (2007), Regional evaporation estimates from flux tower and MODIS satellite data, *Remote Sens. Environ.* **106**, 3, 285–304, DOI: 10.1016/j.rse.2006.07.007.
- Eagleson, P.S. (1994), The evolution of modern hydrology (from watershed to continent in 30 years), *Adv. Water Resour.* **17**, 1–2, 3–18, DOI: 10.1016/0309-1708(94)90019-1.
- Er-Raki, S., A. Chehbouni, G. Boulet, and D.G. Williams (2010), Using the dual approach of FAO-56 for partitioning ET into soil and plant components for olive orchards in a semi-arid region, *Agr. Water Manage.* **97**, 11, 1769–1778, DOI: 10.1016/j.agwat.2010.06.009.
- Paca, V.H., G.E. Espinoza-Dávalos, T.M. Hessels, D.M. Moreira, G.F. Comair, and W.G.M. Bastiaanssen (2019), The spatial variability of actual evapotranspiration across the Amazon River Basin based on remote sensing products validated with flux towers, *Ecol. Process.* **8**, 6, DOI: 10.1186/s13717-019-0158-8.
- Piani, C., J.O. Haerter, and E. Coppola (2010), Statistical bias correction for daily precipitation in regional climate models over Europe, *Theor. Appl. Climatol.* **99**, 187–192, DOI: 10.1007/s00704-009-0134-9.
- Rocha, J., A. Perdigão, R. Melo, and C. Henriques (2010), Managing water in agriculture through remote sensing applications. **In:** R. Reuter (ed.), *Proc. 30th EARSeL Symposium on Remote Sensing for Science, Education, and Natural and Cultural Heritage, Paris, France*, Vol. 31, 223–230, available from: https://www.researchgate.net/profile/Jorge_Rocha7/publication/228413258_Managing_Water_in_Agriculture_through_Remote_Sensing_Applications/links/00b7d533e978b95954000000.pdf.
- Zribi, M., G. Dridi, R. Amri, and Z. Lili-Chabaane (2016), Analysis of the effects of drought on vegetation cover in a Mediterranean Region through the use of SPOT-VGT and TERRA-MODIS long time series, *Remote Sens.* **8**, 12, 992, DOI: 10.3390/rs8120992.

Received 17 November 2022

Accepted 20 December 2022